

THE LIFE CYCLE OF ANTIBODY-FORMING CELLS

I. THE GENERATION TIME OF 19S HEMOLYTIC PLAQUE-FORMING CELLS DURING THE PRIMARY AND SECONDARY RESPONSES*, ‡

BY WALTER J. K. TANNENBERG, M.D., AND ANAND N. MALAVIYA, M.D.

(From the Clinical Immunology Service, New England Medical Center Hospitals and the Department of Medicine, Tufts University School of Medicine, Boston, Massachusetts 02111)

(Received for publication 2 May 1968)

There is a close temporal relationship between the increases in cellular proliferation and antibody synthesis observed when antigen contacts lymphoid tissue (1). Nonetheless, the functional relationship between proliferation and antibody synthesis is ill-defined, even though both activities occur in the same cell (2). It has been proposed that antigen stimulates a small clone of immunologically competent cells both to synthesize antibody and to divide rapidly, producing large numbers of antibody-forming cells within a few days. Support for this hypothesis has been obtained from data showing that, following immunization of mice with sheep red blood cells (SRBC), the number of splenic plaque-forming cells (PFC) doubles every 7 hr during the exponential phase of the response (3, 4). This rapid rate of appearance of PFC has been equated with the rate of proliferation of these cells.

That this need not be a unique interpretation of the data is suggested by studies showing that mouse PFC proliferate at a relatively slow rate, despite their rapid appearance (2). Indeed, in other systems, some workers have found a negative correlation between proliferation and immunological activity (5).

This report is an analysis of the quantitative relationship between the rate of appearance and the rate of proliferation of cells forming 19S hemolytic antibody. The experiments were designed to measure the length of the generation cycle and its subphases in these cells. The results, obtained by radioautographic analysis of over 11,000 PFC, show that the rate of cell proliferation is too slow to account for the rapid appearance of PFC. Mechanisms other than the above hypothesis must therefore be sought to explain the production of antibody-forming cells.

* Presented in part at the 3rd Annual Meeting of the Reticuloendothelial Society, November 1966, and the 50th Annual Meeting of the Federation of American Societies of Experimental Biology, April 1967.

‡ Supported by U. S. Public Health Service Grants AI 07555-01 and AM 07937-04.

Materials and Methods

Mice.—Male C57BL/6J mice between 6 and 8 wk old were used. They received Purina Laboratory Chow and water *ad libitum*.

SRBC.—Sheep blood in Alsever's solution (Colorado Serum Company, Denver, Colo.) was stored at 4°C. not more than 7 days before use. The cells were washed three times and suspended in 0.15 M NaCl just before use.

Thymidine-2-¹⁴C and Thymidine-Methyl-³H.—These were obtained from the New England Nuclear Corporation, Boston, Mass., with specific activities of 30 mc/mm and 6.7 c/mm, respectively, and used within 1 month of receipt.

DEAE Dextran.—This was obtained from Pharmacia Fine Chemicals, Uppsala, Sweden, (mol. wt. 2×10^6). It was dissolved in Tris-HCl buffer, pH 7.2, in a concentration of 2 mg/ml.

Complement.—Dried guinea pig complement (Hyland Laboratories, Los Angeles, Calif.) was reconstituted and diluted 1:2 before use.

Complement Diluent.—This contained 0.15 M NaCl, 0.27 mM CaCl₂, and 0.39 mM MgCl₂.

Slides.—Alcohol-cleaned slides were treated before use by dipping into melted 0.5% agar (Purified Agar, Difco) in water. The agar dried to a thin, hard film that provided a transparent, adhesive surface. The treated slides were numbered and stored for later use.

Immunization.—For the primary response between 1×10^9 and 5×10^9 SRBC were injected intraperitoneally into mice. For studies of the secondary response, mice received two intraperitoneal injections of the same amount of antigen 5 wk apart.

Hemolytic Plaques.—Conventional preparations for assay of the immune responses were made as described by Jerne *et al.* (3), but minor modifications were used in making plaques for radioautography. Mice were killed by cervical dislocation and their spleens were removed, weighed, minced, and gently forced through a fine tantalum wire mesh. The spleen cells were suspended in ice-cold tissue culture medium (TC Medium 858, Difco) within 4 min after sacrifice. They were allowed to settle for a few minutes, the supernatant monodisperse suspension was decanted, and the cells were counted in a hemocytometer. Desiccated TC Medium 858 was dissolved in water just before use, and after adding 0.5% agar and heating, its pH was adjusted to 7.2 with 10% NaHCO₃. To 1 ml of agar solution kept at 45°C. were added in rapid succession: 0.1 ml of DEAE dextran solution, 0.1 ml of 5–10% SRBC, and 0.1 ml of a spleen cell suspension containing between 5×10^9 and 1×10^6 nucleated cells. After rapid mixing, the suspension was poured onto a treated slide in a Petri dish. The dish was rapidly tilted to distribute the suspension and to allow most of it to run off the slide into the dish, leaving but a thin film of the suspension on the slide. The slides were incubated 1 hr at 37°C. in a moist atmosphere. After incubation, excess agar was removed from the back of the slides, the slides were momentarily dipped into complement diluent, and then placed in clean Petri dishes. Two drops of complement were spread evenly on the wet agar and the slides were then incubated for ½ hr at 37°C. 20 ml of phosphate-buffered formalin, pH 7, were added and the slides were fixed overnight. They were washed three times with water to remove salts and were allowed to dry at room temperature.

Radioautography.—Slides bearing hemolytic plaques in which the PFC were labeled *in vivo* were dipped into melted Kodak Nuclear Track Emulsion NTB-2, and exposed in a desiccated atmosphere at –20°C. Exposure times varied between 90 and 400 days. After development in Kodak D-19, fixation and washing, the slides were stained with Giemsa's stain, dried, and stored in a horizontal position until they were read. No cover slips were mounted.

Measurement of the Generation Time of PFC.—This was done by the double-label method developed by Wimber and Quastler (6) in which cells are labeled either with tritium or carbon-14. The different beta particle energies of tritium and carbon-14 enable one to distinguish these isotopes radioautographically (Figs. 7 and 8). The experiment consists of three steps. First, tritium-labeled thymidine (1 μc/g body weight) is injected intraperitoneally (9) into an

immunized mouse, labeling all the PFC that are in the S period at that moment (Fig. 5c). Second, a known time interval is allowed to elapse. During this time, cells continue to move through the generation cycle and some of the tritium-labeled cells move out of the S period (Fig. 5d). Third, the animal is injected intraperitoneally with thymidine-2-¹⁴C (0.3 μ c/g body weight). All the cells in the S period at that moment are now labeled with carbon-14 (Fig. 5d). The tritium-labeled cells that have left the S period can no longer incorporate thymidine and do not become labeled with carbon-14. However, the tritium-labeled cells still in the S period now have a carbon label obscuring the tritium label and these cells will be scored as carbon-labeled cells (Fig. 8). 30 min later, the animal is killed, hemolytic plaques are made, and the preparations are radioautographed. The antigen and the thymidine were injected at a time of day such that the animals could always be sacrificed between 10 a.m. and noon to minimize possible effects of diurnal variation on the generation cycle (10, 11). The times were also chosen so that sacrifice occurred during the exponential portion of the PFC response, as indicated by the bars in Fig. 1.

Scoring of Labeled PFC.—The total area of all slides was examined under magnification of 40 and all PFC were identified by their central position in hemolytic plaques. Individual PFC were then examined under magnification of 1000 and scored as being unlabeled, or labeled either with tritium or carbon-14. PFC in which no decision could be made for any reason were allotted to a separate category. The labeling scores were used to calculate the generation time by the equations described in the Appendix.

RESULTS

Rate of Appearance of PFC.—Groups of 4–10 mice were sacrificed at various intervals after primary or secondary immunization and conventional hemolytic plaque assays were made of the spleen cells. The results are shown in Fig. 1. The assay method is insufficiently sensitive to detect an increase in PFC above background levels until about 24 hr after immunization. The curve then rises exponentially to a peak at about 96 hr during the primary response, with a doubling time of about 7 hr. During the secondary response, the peak occurs at about 84 hr, with a doubling time of about 6 hr.

The rate at which PFC appear has been shown to be dependent on the dose of antigen (3, 12). Preliminary experiments showed that the amount of antigen used (between 1×10^9 and 5×10^9 SRBC) was about a 100-fold excess of that required for the maximum rate of response, and that this dose did not change the rate or the magnitude of the maximum PFC response. 5 wk after primary immunization with this dose, the number of PFC had fallen to the background levels present before the primary response.

Estimation of the Generation Time of PFC during the "Log Phase".—The PFC radioautographic scores are shown in Table I for the primary response and in Table II for the secondary response. Usually less than 2% of all PFC could not be definitely assigned to one of the three scoring categories. The labeling scores were independent of the number of such equivocal PFC, which were therefore ignored in the calculations. Labeling was generally intense compared to background radiation; there was no significant difference in scores of radioautographs exposed for 90 or 400 days. Conventional PFC assays were also

made from the same spleen samples; these showed no significant difference from the data in Fig. 1.

The numbers of PFC scored in each category were inserted into Equations (1) and (2) and the duration of the S period and of the total generation time were calculated. Since these equations are valid only when the isotope intervals are short, only data obtained with intervals of 1–4 hr were used in these calcu-

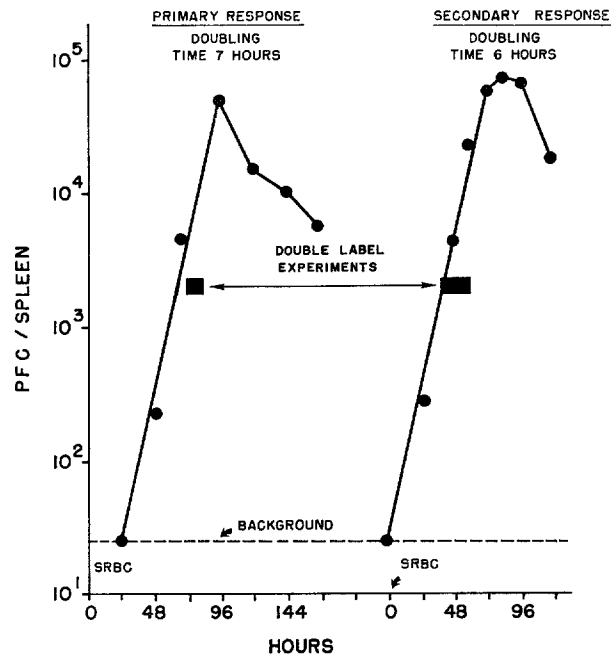


FIG. 1. Rate of appearance of plaque-forming cells. Mice were immunized with SRBC at the times shown. Each point is the mean of 4–10 mice. The mice shown here were not given radioisotopes. The bars indicate the periods in which the double label experiments were done on the mice listed in Tables I and II. The secondary challenge was 5 wk after the primary.

lations. The results are shown in Table III. During the exponential portions of the PFC response shown in Fig. 1, the length of the S period was about 8 hr and the length of the total generation cycle was slightly more than 13 hr in both the primary and the secondary responses.

Graphical Estimate of the Generation Time.—Additional experiments were done to confirm the length of the generation cycle during the exponential phase of the immune response. The intervals between the isotope injections were extended and the animals were killed 84 hr or 60 hr after the primary and secondary challenges, respectively. The ratio H/C was plotted as a function of the isotope interval in Fig. 2. As shown in Fig. 6, this ratio becomes zero

when the isotope interval equals the generation time. Fig. 2 indicates that these curves intersect the time axis between 13 and 14 hr. This confirms the values calculated by Equation (2) for mice killed 84 hr or 60 hr after the primary and secondary challenges, respectively.

TABLE I
PFC Labeling Scores in the Primary Response

Time of sacrifice after challenge	Isotope interval	Number of ³ H PFC	Number of ¹⁴ C PFC	Number of unlabeled PFC
<i>hr</i>	<i>hr</i>			
84*	1*	11*	75*	36*
84	1	14	145	79
84	1	38	204	110
84	1	18	179	66
84	2	30	123	203
84	2	31	127	194
84	2	15	66	27
84	3	11	52	6
84	3	6	19	7
84	3	31	94	18
84	3	43	101	27
84	4	40	81	2
84	4	56	138	13
84	4	25	63	3
84	5	36	97	8
84	5	80	175	15
84	7	39	54	5
84	7	26	36	4
84	8	5	8	1
84	8	21	33	3
84	8	13	27	0
84	12	10	32	18
84	12	32	107	66
84	12	16	114	51
84	12	2	9	6

* Each horizontal row gives the data from a single mouse.

Estimation of the Length of G-2 and G-1.—The duration of G-2 was determined by noting the earliest isotope interval at which labeled mitotic figures can be observed. This occurred at an interval of 2 hr; none were seen at 1 hr (Fig. 7). Subtracting the sum of G-2 (2 hr) and S (8 hr) from the generation time (13 hr), the length of G-1 is about 3 hr. The duration of mitosis could not be estimated from our data. McFarland et al. (13) found that cytokinesis of lymphocytes required about 5 min while Clafin and Smithies (14), observing a single PFC, estimated the total duration of mitosis to be about 40 min. In all our calculations we have ignored these short intervals.

TABLE II
PFC Labeling Scores in the Secondary Response

Time of sacrifice after challenge	Isotope interval	Number of ³ H PFC	Number of ¹⁴ C PFC	Number of unlabeled PFC
<i>hr</i>	<i>hr</i>			
48*	2*	6*	16*	9*
48	2	13	52	12
48	2	20	76	19
48	2	13	53	34
60	1	9	58	53
60	1	5	42	30
60	1	5	38	31
60	1	4	23	17
60	2	17	72	37
60	2	12	44	24
60	2	8	32	13
60	2	12	45	22
60	2	16	57	19
60	2	6	24	14
60	2	16	57	34
60	2	7	25	11
60	3	20	46	20
60	3	27	68	31
60	3	25	88	35
60	3	24	63	36
60	4	34	63	22
60	4	14	25	7
60	4	34	66	14
60	5	25	75	9
60	5	35	66	10
60	5	38	55	8
60	6	77	161	18
60	6	32	52	11
60	6	54	62	37
60	6	48	87	11

Evidence of Asynchrony in the PFC Population.—Fig. 2 shows that a substantial degree of asynchrony exists at all isotope intervals (i.e., between midnight and noon). Were the PFC population synchronized, the H/C ratio could not vary as shown because either the numerator or the denominator of the ratio would always be zero. Many factors may have caused the observed deviations from the theoretical H/C curves, including small tendencies towards synchrony produced by antigen administration or diurnal effects, but these appear to be negligible.

In an asynchronous population the probability of finding a cell in the S

TABLE II—*Concluded*

Time of sacrifice after challenge	Isotope interval	Number of ³ H PFC	Number of ¹⁴ C PFC	Number of unlabeled PFC
<i>hr</i>	<i>hr</i>			
60*	6*	35*	50*	8*
60	7	88	150	22
60	7	34	73	10
60	7	52	71	6
60	8	58	103	3
60	8	46	53	3
60	8	52	66	3
60	8	48	62	5
60	11	36	87	30
60	11	24	65	15
60	11	13	34	21
60	11	22	66	29
60	2	23‡	75	40
60	2	18‡	71	38
60	2	45‡	170	102
60	2	31§	113	47
60	2	22§	86	33
60	2	24§	81	46
60	2	19§	82	38
60	2	61	232	84
60	2	22	70	38
60	2	16	64	45
60	2	19	67	49
60	2	17¶	61	40
60	2	53¶	200	92
60	2	23¶	89	40
60	2	18¶	72	31

* Each horizontal row gives the data from a single mouse.

‡ 2 μ C/g body weight of thymidine-methyl-³H.

§ 4 μ C/g body weight of thymidine-methyl-³H.

|| 8 μ C/g body weight of thymidine-methyl-³H.

¶ 16 μ C/g body weight of thymidine-methyl-³H.

period is constant and equal to the ratio of carbon-labeled cells to the total population sample (Equation 2). Since carbon-labeled thymidine was given at the end of the experiment (about noon-time), the carbon-labeling index can only give a spot check on asynchrony at that time of day. In 25 mice examined during the primary response, (Table I) the carbon-labeling index was 0.59 ± 0.09 (SD), and in 57 mice studied during the secondary response (Table II), the index was 0.56 ± 0.05 (SD). The small variances indicate asynchrony, for if the cell populations were synchronized, these indices would be expected

to vary uniformly from 0 to 1.0. Although neither complete synchrony nor complete asynchrony are generally found in vivo, we conclude that these data show a sufficient degree of asynchrony to validate the method.

Evidence of Negligible Variation of the Generation Time.—Cell populations highly uniform by most criteria still contain a small percentage of cells with generation times significantly different from the mean (15, 16). This was evaluated by comparing the behavior of PFC with that expected of a perfectly uniform population. As shown in Fig. 5 c-5 f, when the isotope interval equals $G-1 + G-2$, these periods are filled with tritium-labeled cells. The S period is then filled with carbon-labeled cells. No unlabeled cells should be found when the isotope interval is about 5 hr ($g_1 + g_2$). Fig. 3 shows that the sum of the

TABLE III
*The Duration of the Generation Cycle and The S Period of Mouse 19S PFC**

Time of assay after challenge	Number of mice†	S Period	Generation cycle
hr		hr ± SE	hr ± SE
<i>Primary response</i>			
84	14	8.1 ± 0.6	13.0 ± 0.4
<i>Secondary response</i>			
48	4	7.2 ± 0.6	12.2 ± 1.1
60	19	7.4 ± 0.2	13.6 ± 0.6

* Calculated with Equations (1) and (2), using data in Tables I and II.

† Only mice with isotope intervals of 1-4 hr were used in these calculations.

tritium and carbon scores very nearly equals 100% at the expected time. The closeness of the curve to the expected value indicates that any subpopulations of PFC with generation times differing from the mean are small in size.

Efficiency of Detection of Tritium-Labeled Cells.—The number of tritium-labeled cells observed may not be equal to the number of cells actually labeled with tritium because the thickness of agar that lies between the labeled nucleus and the photographic emulsion might exceed the range of tritium beta particles (mean range 1 μ , maximum 6 μ in water (17-19); the range in dried agar is not known).

Three methods were used to estimate the thickness of the preparations. The focusing method of Lange and Engström (20) gave a mean thickness over 20 consecutive PFC of 0.5 μ ; this equals the theoretical resolution of the microscope and thereby lacks precision and accuracy. The total area of the agar-cell sheet was measured on 10 consecutive slides. The material was scraped off and its mass, density, and volume determined. Assuming the sheet to be a rectangular parallelepiped, its mean thickness was calculated from its area and volume to be 2.0 $\mu \pm 0.7$ (SD). When a few samples were prepared on a reflecting

surface, instead of transparent glass slides, observation of the colored interference patterns gave a maximum thickness of 0.8μ . It seems unlikely that distances of this approximate magnitude would cause 100% attenuation of tritium

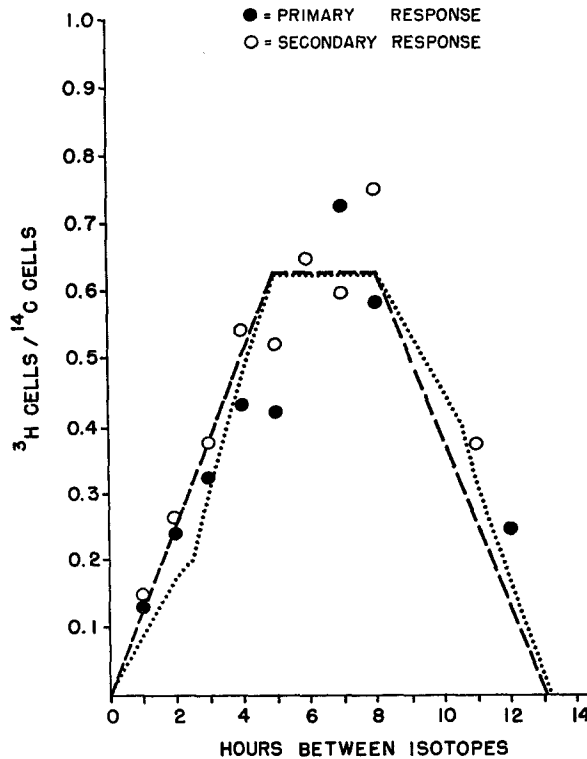


FIG. 2. Experimental ratio of tritium-labeled cells to carbon-labeled cells as a function of the isotope interval. Each point is the mean of the mice given the two isotope injections as listed in Tables I and II. The ratio H/C was calculated from the PFC labeling scores shown in Tables I and II. The dashed line indicates the theoretical steady-state curve and the dotted line indicates the theoretical exponential growth curve in which $G-1 = G-2$; both curves are the same as shown in Fig. 6. The experimental data are not precise enough to fit either theoretical curve to the exclusion of the other. The data do exclude the theoretical curves in which either $G-1$ or $G-2$ are zero. Note that, regardless of the ultimate shape of the curve, it returns to zero between 13 and 14 hr, confirming the calculation of the generation time in Table III.

particles; lesser degrees of attenuation would result in detection of the tritium label.

Fig. 3 shows a more functional approach to the accuracy of tritium scoring by showing that almost all PFC are labeled at the expected times. The failure of the curve to reach 100% is due to the sum of all systematic errors, including

flaws in tritium scoring and variations in the generation time. The graph closely approaches 100% and shows that these errors are acceptably small. In another experiment, a few mice were given two injections of thymidine- ^{14}C at the same intervals usually used for the tritium-carbon injections. Assuming the energy of carbon-14 is sufficient to assure detection of all carbon-labeled cells, the total number of carbon-labeled cells should equal the sum of the tritium and carbon scores found at the same intervals. Fig. 3 shows that the detection

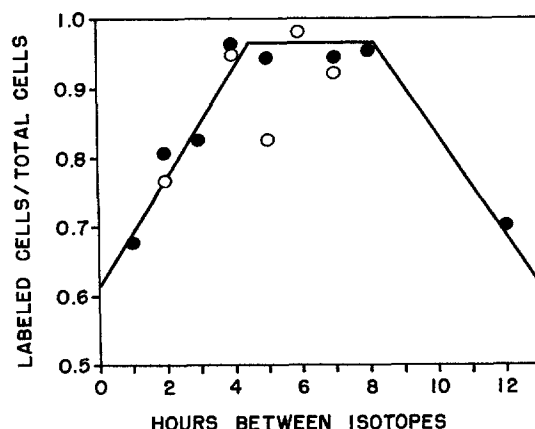


FIG. 3. The fraction of labeled PFC as a function of the isotope interval. The solid circles are the mean of mice killed 84 hr after primary immunization and injected with thymidine- ^3H and ^{14}C at the intervals shown. The number of labeled cells is the sum of the tritium and carbon scores for each animal in Table I; the total number of cells is the sum of the labeled cells and the unlabeled cells. The open circles indicate single mice given two injections of thymidine- ^{14}C at the intervals shown, and killed 84 hr after the primary challenge. Theory predicts that the curve should reach a maximum of 1.0 when the isotope interval equals the sum of G-1 and G-2.

efficiency is essentially the same in both the carbon-carbon and tritium-carbon runs.

A final control is found by comparing the results of Equations (1) and (2) in Table III with the results of Fig. 2. Insertion of falsely low tritium scores into Equations (1) and (2) will yield an *overestimation* of the duration of the generation time. However, the same falsely low values plotted as in Fig. 2 will lead to an *underestimation* of the generation time. As shown above, no discrepancy occurs between the two methods. From these lines of evidence, we conclude there were no significant errors in the detection of tritium-labeled cells.

Effect of Intranuclear Radiation on the Generation Time.—Radiation from the isotopes used in the determination of the generation cycle may change the length of the cycle (6, 21–23). This possibility was studied only in the case of tritium-labeled thymidine because the PFC were exposed to this isotope far

longer than to carbon-14 and because tritium radiation is absorbed mostly in the nucleus, in contrast to carbon-14 (17, 18).

If tritium did change the length of the cycle, it would be expected that this effect should be dose-related. This was tested by using doses of tritium much higher than the standard dose of 1 $\mu\text{C/g}$ body weight that was used in all the experiments reported above. The usual dose of carbon-14 was given, the time interval between isotope injections was two hours in all cases, the animals were killed 60 hr after secondary challenge, and the plaque preparations, scoring, and calculations were done as before. Table IV shows that neither the length of the S period nor that of the generation cycle changed significantly when PFC were exposed in vivo to high doses of tritium for 2 hr. We conclude

TABLE IV
Effect of Tritium Radiation on the Generation Cycle

^3H injected i.p.*	Number of mice†	S period‡	Generation cycle§
$\mu\text{C/g}$ body wt		hr \pm SE	hr \pm SE
1	19	7.4 \pm 0.2	13.6 \pm 0.6
2	3	7.3 \pm 0.3	13.3 \pm 0.4
4	4	7.5 \pm 0.3	13.0 \pm 0.5
8	4	7.2 \pm 0.4	13.4 \pm 0.9
16	4	7.5 \pm 0.2	13.3 \pm 0.2

* Given as thymidine-methyl- ^3H as described in the text.

† All mice were killed 60 hr after the secondary challenge.

‡ Calculated with Equations (1) and (2), using the PFC-labeling scores in Table II.

that the tritium dose usually given, 1 $\mu\text{C/g}$ body weight, does not introduce errors into the data derived from the short term experiments, and probably does not do so when exposures are extended up to a single generation cycle.

DISCUSSION

Validity of the Experimental Methods.—

1. *Is the theoretical derivation valid?* Of the four assumptions demanded by Wimber and Quastler (6), we have shown asynchrony and a negligible variation in the population's generation time. In the absence of a formal proof of the steady state or exponential nature of PFC kinetics, the double label technique has been expanded and shown to be valid in all cases (Fig. 6).

2. *Does radioactive thymidine alter the system?* Table IV shows that the doses of tritium used in this work do not alter the results when the in vivo exposure is limited to 2 hr. The consistency of the data found at longer isotope intervals (Fig. 2) with those at 2 hr intervals indicates that 1 $\mu\text{C/g}$ body weight has no measurable effect during any of the in vivo exposure times used. Similar conclusions were reached by others using radiosensitive cell systems (24-26).

Puck (21) and others (27) have suggested that exogenous thymidine may influence the generation cycle, but Table IV shows that this did not occur in this system.

3. *Does radioactive thymidine label cells in the manner assumed?* The use of labeled thymidine is usually based on the premises that the material is incorporated into DNA within a few minutes of injection (28), that only DNA is labeled (29), that the isotope is chemically stable in thymidine, that the DNA is metabolically stable, and that the label is not reutilized after cell death. Some of these premises have been challenged. Several reports (30-32) have shown that labeled thymidine may be available for incorporation for extended periods. If tritiated thymidine were continuously incorporated during the interval between isotope injections, the unlabeled cells that enter the S period from G-1, (Fig. 5 d) would be labeled. This is of no consequence because these "extra" tritium-labeled cells will be relabeled with carbon-14 and so scored, as they are in any event. The persistent incorporation of thymidine-2-¹⁴C is halted when the experiment is terminated by chilling and dilution of the spleen cells. We have not examined the possibility of reutilization of labeled DNA (33-35), but since the interval studied was no longer than one generation cycle, we assume that only a small number of cells died in any tissue and contributed negligible label to the PFC. Labeled thymidine might enter mitochondrial DNA (36), but we ignore this as being very small compared to the nuclear DNA.

4. *Do the PFC define a population synthesizing 19S antibody?* Direct evidence that the PFC described here actually produce 19S antibody is lacking. We assume, as do others (37), that the concordant increases in the number of PFC and in the titer of serum 19S antibody is the best available evidence for the nature of the hemolytic antibody synthesized by these cells.

Previous Estimates of the Generation Time of Antibody-Forming cells: In support of the data on mouse PFC, it is of interest that the duration of the S period has been found to be constant in all mouse tissues studied. It lasts 7 to 9 hr regardless of the length of the total generation cycle, which may vary from 16 to 181 hr (38-42). This is in good agreement with the S period data in Table III.

Previous efforts to measure the proliferation of specific antibody-forming cells have yielded conflicting results. Baney, Vazquez, and Dixon (43) studied antibody-forming cells during the secondary response by injecting rabbits with tritiated thymidine every 6 hr between antigenic challenge and sacrifice, 4 days later. Using specific immunofluorescence and radioautography sequentially on the same cells, 92% of cells containing specific antibody were found to be labeled. These findings are consistent with ours, for repeated injections of labeled thymidine at intervals equal to or less than the length of the S period will label all cells in the population (Fig. 3).

Koros, Fuji, and Jerne (44) suggested that the doubling time of mouse PFC

was equal to their generation time. After giving a single pulse of tritiated thymidine, they found that the PFC labeling index was 55%. This agrees well with the carbon-labeling index reported here of 0.59 ± 0.09 , but these data alone are insufficient to support the authors' hypothesis.

Rowley et al. studied the primary PFC response of rats with a novel method for estimating the cell generation time (45).¹ They found that during the exponential phase of the response the generation time is equal to the doubling time of 5–8 hr. Their results are in profound conflict with ours; resolution of this discrepancy must await a critical evaluation of the techniques used in each laboratory.

Many other workers have estimated cell generation times in lymphoid tissues during the immune response (46–58). Their experiments differ from ours and those quoted above in one major technical element: determinations of the generation time and of antibody-forming capacity were not made simultaneously on the same cells; but rather, the data were gathered by observing changes in morphological classes of cells in sections or smears. The value of these reports is thus diminished by the failure to study a functionally homogenous cell population.

Significance of the Results.—Two points seem manifest. First, virtually all PFC synthesize DNA, confirming previous work (2, 43, 59, 60). Second, the generation time of PFC is about 13 hr during the early primary and secondary immune responses at points when the number of PFC doubles every 6 to 7 hr. The doubling time, therefore, is not a measure of the generation time (61). This observation makes untenable the hypothesis that the rate of appearance of PFC is their rate of proliferation. Any relation between these two rates, if present, is not apparent.

Another interpretation of the kinetics of the splenic PFC response is therefore necessary. We will ignore the possibility that the rate of appearance of PFC depends on the rate of cell migration to the spleen, since Mishell and Dutton (62) showed that spleen cells alone yield in vitro responses equal to those of the intact animal.

A number of workers have proposed that the PFC response reflects the rate of induction of antibody synthesis in immunocompetent cells by antigen (2, 63–66). Such a mechanism requires a large initial clone (67), its size far exceeding that estimated by extrapolating the curves in Fig. 1 to zero time. It may seem paradoxical to suggest that differentiation is the major factor in the production of PFC, when all the data show that they are proliferating, but a change in emphasis may clarify the problem. The question is not *whether* PFC proliferate, for they certainly do. The question, rather, is *how* do PFC proliferate.

The Appendix shows that real cell population kinetics probably lie between

¹ We wish to acknowledge the kindness of the authors in allowing us to study their manuscript before its publication.

two limiting, ideal models of growth: exponential and the steady-state. The relatively long generation time indicates that even if exponential growth were to occur, the number of cells so produced would make but a small contribution to the total actually observed. For this reason, we propose the hypothesis that the PFC proliferate with steady-state kinetics; for speculative purposes it may be useful to reject the notion of exponential growth which, previously, has been tacitly assumed.

As shown in Fig. 4, steady-state cell proliferation would prepare the animal for further immune responses by replacing the original immunocompetent

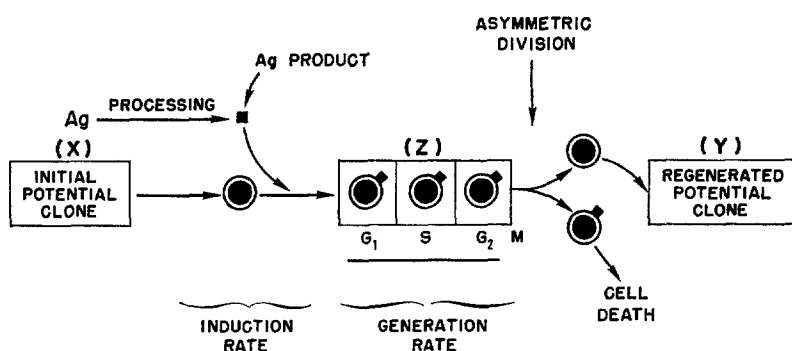


FIG. 4. Hypothetical steady-state. Hypothetical scheme devised to reconcile the observed rate of appearance of PFC with the observed rate of proliferation. The rate of appearance of PFC (Fig. 1) is the induction rate, above. This rate is independent of the generation rate of PFC. Proliferation is assumed to be in the steady-state. Asymmetric division occurs when the antigen product is donated to only one of the two cells produced at mitosis. The cell with the antigen product continues to synthesize antibody for a time and ultimately dies. The cell lacking the antigen product replaces the member of the original immunocompetent clone initially induced to activity. X, Y, and Z refer to the XYZ nomenclature (71).

clone; it would not increase the number of antibody-forming cells. Replacement from *some* source appears necessary in any event, for it is believed that when antibody-forming cells become highly differentiated they ultimately die (56, 61, 68, 69). Since PFC become increasingly differentiated during the immune response (70), they may suffer such a fate.

Fig. 4 also shows that, although the induction rate of PFC is independent of their generation rate, both these rates are essential elements of the immune response. The induction rate reflects the rate at which X cells (71) are stimulated to enter both antibody synthesis and the start of proliferation. We further propose that the rate of induction is controlled by the rate at which antigen is processed, perhaps by macrophages, into a suitable antigen product such as antigen fragments or macrophage RNA (72). It is this final product that stimulates the X cell at the rate shown in Fig. 1. Bearing the antigen product, the

cell enters the generation cycle at G-1 (73). When it reaches mitosis, the antigen product, assumed to be necessary for continuing antibody synthesis, is donated to only one of the two daughter cells. This is because a mechanism by which antigen fragments, or macrophage RNA, could be replicated in the antibody-forming cell seems unlikely. As a consequence, cell division is asymmetric, as proposed by Makinodan and Albright (68) and Talmage and Claman (74). Asymmetric division, which occurs in all multicellular organisms, implies an unequal distribution of somatic potential (e.g., antigen product); it is assumed that the genetic potential is always equally shared. The general mechanism by which somatic potential is unequally divided is unknown. In PFC this could occur if but a single unit of antigen product (or conversely, a single receptor site) were present on the cell. The amount of antigen on the cell may be below the limits of detection by available methods and could account for the failure of Nossal et al. (75) to detect antigen in antibody-forming cells. Sercarz and Byers (71) also proposed a limited number of receptor sites on such cells.

After asymmetric division in the steady state, the cell bearing the antigen product continues to differentiate and to synthesize antibody. It ultimately dies. The second daughter cell, however, lacks the nonreplicating antigen product and is no longer stimulated to make antibody. Antibody synthesis or excretion may continue in this cell for a short time after mitosis, as shown by Claffin and Smithies (14), but it should eventually cease in the absence of a stimulus (76). This cell, differentiating no further, does not die. It has all the characteristics of the original immunocompetent cell plus recent antigenic experience, and corresponds to the Y cell (71). It is available for stimulation with more antigen product; if antigen is given during the primary response, this cell may represent the "net-excess" response (71, 77); if antigen is given later, it is responsible for the 19S secondary response (Fig. 1). The hypothesis also suggests that these replacement cells should remain labeled if radioactive thymidine is injected while they are passing through the cycle. Miller (78) has found labeled immunocompetent cells up to 6 months after injection of the label.

Fig. 4 shows that the steady-state mechanism results in a one-for-one replacement of the original, induced, and doomed clone if each PFC passed through the generation cycle but once. If the PFC passed through the cycle twice, the maximum we have suggested earlier (2), then the clone available for the anamnestic response would be twice as large as the original clone, neglecting any attrition. The magnitude of the secondary response of 19S cells generally lies between these two limits (79) (Fig. 1).

SUMMARY

The generation time of cells synthesizing 19S antibody was measured during the exponential phase of the primary and secondary immune responses. Using

a plaque-forming cell assay together with a double label isotope method, the duration of the generation time was found to be about 13 hr, that of the S period was about 8 hr, and that of G-1 and G-2 were about 3 and 2 hr, respectively, in both immune responses.

Previous work was confirmed showing that all plaque-forming cells observed during the exponential phase of the immune responses incorporate labeled thymidine, and therefore take part in proliferation.

These results were obtained at points during both responses when the doubling time of the PFC was observed to be 6-7 hr. This finding makes untenable the hypothesis that the rate of appearance of PFC equals the rate of proliferation of these cells.

A hypothesis is presented to account for these findings and to serve as a basis for further experiments.

BIBLIOGRAPHY

1. Ehrlich, W. E., D. L. Drabkin, and C. Forman. 1949. Nucleic acids and the production of antibody by plasma cells. *J. Exptl. Med.* **90**:157.
2. Tannenber, W. J. K. 1967. Induction of 19S antibody synthesis without stimulation of cellular proliferation. *Nature.* **214**:293.
3. Jerne, N. K., A. A. Nordin, and C. Henry. 1963. The agar plaque technique for recognizing antibody-producing cells. *In* Cell-Bound Antibodies. B. Amos and H. Koprowski, editors. The Wistar Institute Press, Philadelphia. 109.
4. Hege, J. S., and L. J. Cole. 1966. Antibody plaque-forming cells: Kinetics of the primary and secondary responses. *J. Immunol.* **96**:559.
5. Nisbert, N. W., and M. Simonsen. 1967. Primary immune response in grafted cells. Dissociation between the proliferation of activity and the proliferation of cells. *J. Exptl. Med.* **125**:967.
6. Wimber, D. E., and H. Quastler. 1963. A ¹⁴C- and ³H-thymidine double labeling technique in the study of cell proliferation in *Tradescantia* root tips. *Exptl. Cell Res.* **30**:8.
7. Hughes, W. L., V. P. Bond, G. Brecher, E. P. Cronkite, R. B. Painter, H. Quastler, and F. G. Sherman. 1958. Cellular proliferation in the mouse as revealed by autoradiography with tritiated thymidine. *Proc. Nat. Acad. Sci. U. S.* **44**:476.
8. Dawson, K. B., and E. O. Field. 1964. A procedure for computing cellular proliferation kinetics during "log phase" of growth. *Exptl. Cell Res.* **34**:507.
9. Petersen, R. O., and R. Baserga. 1964. Route of injection and uptake of tritiated precursors. *Arch. Pathol.* **77**:582.
10. Bullough, W. S. 1948. Mitotic activity in the adult male mouse, *Mus musculus* L. The diurnal cycles and their relation to waking and sleeping. *Proc. Roy. Soc. (London), Ser. B*: **135**:212.
11. Hinrichs, H. R., R. O. Petersen, and R. Baserga. 1964. Incorporation of thymidine into DNA of mouse organs. *Arch. Path.* **78**:245.
12. Wortis, H. H., R. B. Taylor, and W. D. Dresser. 1966. Antibody production studied by means of the LHG assay. I. The splenic response of CBA mice to sheep erythrocytes. *Immunology.* **11**:603.

13. McFarland, W., D. H. Heilman, and J. F. Moorhead. 1966. Functional anatomy of the lymphocyte in immunological reactions in vitro. *J. Exptl. Med.* **124**:851.
14. Clafin, A. J., and O. Smithies. 1967. Antibody-producing cells in division. *Science*. **157**:1561.
15. Mendelsohn, M. L. 1962. Chronic infusion of tritiated thymidine into mice with tumors. *Science*. **135**:213.
16. Drew, R. M., and R. B. Painter. 1962. Further studies on the clonal growth of HeLa S3 cells treated with tritiated thymidine. *Radiation Res.* **16**:303.
17. Stewart, F. S. 1964. The calculation of radiation dose from distributed sources of tritium. *Intern. J. Radiation Biol.* **8**:545.
18. Apelgot, S., and M. Duquesne. 1964. Energie dissipée par le tritium dans des microorganismes. *Intern. J. Radiation Biol.* **7**:65.
19. Robertson, J. S., V. P. Bond, and E. P. Cronkite. 1959. Resolution and image spread in autoradiography of tritium-labeled cells. *Intern. J. Appl. Radiation.* **7**:33.
20. Lange, P. W., and A. Engström. 1954. Determination of thickness of microscopic objects. *Lab. Invest.* **3**:116.
21. Puck, T. T. 1964. Studies of the life cycle of mammalian cells. *Cold Spring Harbor Symp. Quant. Biol.* **29**:167.
22. Wimber, D. E., and L. F. Lamerton. 1966. Cell population kinetics in the intestine of continuously irradiated mice, using double-labelling autoradiography. *Radiation Res.* **28**:694.
23. Wimber, D. E. 1966. Prolongation of the cell cycle in *Tradescantia* root tips by continuous gamma irradiation. *Exptl. Cell Res.* **42**:296.
24. Fry, R. J. M., S. Leshner, and H. I. Kohn. 1961. Estimation of time of generation of living cells. *Nature*. **191**:290.
25. Johnson, H. A., and E. P. Cronkite. 1959. The effect of tritiated thymidine on mouse spermatogonia. *Radiation Res.* **11**:825.
26. Steel, G. G., and L. F. Lamerton. 1965. The turnover of tritium from thymidine in tissues of the rat. *Exptl. Cell Res.* **37**:117.
27. Greulich, R. C., I. L. Cameron, and J. B. Thrasher. 1961. Stimulation of mitosis in adult mice by administration of thymidine. *Proc. Nat. Acad. Sci. U. S.* **47**:743.
28. Rubini, J. R., E. P. Cronkite, V. P. Bond, and T. M. Fliedner. 1960. The metabolism and fate of tritiated thymidine in man. *J. Clin. Invest.* **39**:909.
29. Amano, M., B. Messier, and C. P. Leblond. 1959. Specificity of labelled thymidine as a deoxyribonucleic acid precursor in radioautography. *J. Histochem. Cytochem.* **7**:153.
30. Robinson, S. H., and G. Brecher. 1963. Delayed incorporation of tritiated thymidine into DNA. *Science*. **142**:392.
31. Cleaver, J. E., and R. M. Holford. 1965. Investigation into the incorporation of ³H-thymidine into DNA in L-strain cells and the formation of a pool of phosphorylated derivatives during pulse labeling. *Biochim. Biophys. Acta.* **103**:654.
32. Staroscik, R. N., W. H. Jenkins, and M. L. Mendelsohn. 1964. Availability of tritiated thymidine after intravenous administration. *Nature*. **202**:456.

33. Rieke, W. O. 1962. The *in vivo* reutilization of lymphocytic and sarcoma DNA by cells growing in the peritoneal cavity. *J. Cell Biol.* **13**:205.
34. Hill, M. 1962. Intercellular passage of tritium-thymidine-labelled DNA from donor lymphocytes to recipient bone marrow cells. *Exptl. Cell Res.* **28**:2.
35. Craddock, C. G., G. S. Nakai, H. Fukuta, and L. M. Vauslager. 1964. Proliferative activity of the lymphatic tissues of rats as studied with tritium-labeled thymidine. *J. Exptl. Med.* **120**:389.
36. Nass, M. M. K., S. Nass, and B. A. Afzelius. 1965. The general occurrence of mitochondrial DNA. *Exptl. Cell Res.* **37**:516.
37. Wigzell, H., G. Möller, and B. Andersson. 1966. Studies at the cellular level of the 19S immune response. *Acta Pathol. Microbiol. Scand.* **66**:530.
38. Defendi, V., and L. A. Manson. 1963. Analysis of the life-cycle in mammalian cells. *Nature.* **198**:359.
39. Cameron, I. L., and R. C. Greulich. 1963. Evidence for an essentially constant duration of DNA synthesis in renewing epithelia of the adult mouse. *J. Cell Biol.* **18**:31.
40. Pilgrim, C., W. Erb, and W. Maurer. 1963. Diurnal fluctuations in numbers of DNA synthesizing nuclei in various mouse tissues. *Nature.* **199**:863.
41. Koburg, E., and W. Maurer. 1962. Autoradiographische Untersuchungen mit H-3-Thymidin über die Dauer der DNS-Synthese und ihren zeitlichen Verlauf bei den Darmepithelien und andern Zelltypen der Mause. *Biochim. Biophys. Acta.* **61**:229.
42. Koburg, E. 1963. The use of grain counts in the study of cell proliferation. *In Cell Proliferation*. L. F. Lamerton and R. J. M. Fry, editors. F. A. Davis Company, Philadelphia. 62.
43. Baney, R. N., J. J. Vazquez, and F. J. Dixon. 1962. Cellular proliferation in relation to antibody synthesis. *Proc. Soc. Exptl. Biol. Med.* **109**:1.
44. Koros, A. M. C., H. Fuji, and N. K. Jerne. 1966. Kinetics of proliferation of clones of antibody-producing cells. *Federation. Proc.* **25**:305. (abstract).
45. Rowley, D. A., F. W. Fitch, D. E. Mosier, S. Solliday, L. W. Coppleson, and B. W. Brown. 1968. The rate of division of antibody-forming cells during the early primary immune response. *J. Exptl. Med.* **127**:987.
46. Schooley, J. C. 1961. Autoradiographic observations of plasma cell formation. *J. Immunol.* **86**:331.
47. Urso, P., and T. Makinodan. 1961. Significance of mitosis and maturation in the secondary precipitin response. *Federation Proc.* **20**:25. (abstract).
48. Capalbo, E. E., T. Makinodan, and D. E. Gude. 1962. Fate of H³-thymidine-labeled spleen cells in *in vivo* cultures during the secondary antibody response. *J. Immunol.* **89**:1.
49. Nossal, G. J. V., and O. Mäkelä. 1962. Autoradiographic studies on the immune response. I. The kinetics of plasma cell proliferation. *J. Exptl. Med.* **115**:209.
50. Mäkelä, O., and G. J. V. Nossal. 1962. Autoradiographic studies on the immune response. II. DNA synthesis amongst single antibody-producing cells. *J. Exptl. Med.* **115**:231.
51. Urso, P. and T. Makinodan. 1963. The roles of cellular division and maturation in the formation of precipitating antibody. *J. Immunol.* **90**:897.

52. Capalbo, E. E., and T. Makinodan. 1964. Doubling time of mouse spleen cells during the latent and log phases of the primary antibody response. *J. Immunol.* **92**:234.
53. Nettesheim, P., and T. Makinodan. 1965. Differentiation of lymphocytes undergoing an immune response in diffusion chambers. *J. Immunol.* **94**:868.
54. Olson, G. B., and B. S. Wostmann. 1966. Lymphocytopoiesis, plasmacytopoiesis and cellular proliferation in nonantigenically stimulated germ free mice. *J. Immunol.* **97**:267.
55. Olson, G. B., and B. S. Wostmann. 1966. Cellular and humoral immune response of germ free mice stimulated with 7S HGG or *Salmonella typhimurium*. *J. Immunol.* **97**:275.
56. Balfour, B. M., E. H. Cooper, and E. L. Alpen. 1965. Morphological and kinetic studies on antibody-producing cells in rat lymph nodes. *Immunology.* **8**:230.
57. Sainte-Marie, G., and A. H. Coons. 1964. Studies on antibody production. X. Mode of formation of plasmocytes in cell transfer experiments. *J. Exptl. Med.* **119**:743.
58. Nossal, G. J. V., J. Mitchell, and W. McDonald. 1963. Autoradiographic studies on the immune response. IV. Single cell studies on the primary response. *Australian J. Exptl. Biol. Med. Sci.* **41**:423.
59. Szenberg, A., and A. J. Cunningham. 1968. DNA synthesis in the development of antibody-forming cells during the early stages of the immune response. *Nature.* **217**:747.
60. Dutton, R. W., and R. I. Mishell. 1967. Cell populations and cell proliferation in the in vitro response of normal mouse spleen to heterologous erythrocytes. *J. Exptl. Med.* **126**:443.
61. Makinodan, T., and J. F. Albright. 1967. Proliferative and differentiative manifestations of cellular immune potential. *Progr. Allergy.* **10**:1.
62. Mishell, R. I., and R. W. Dutton. 1967. Immunization of dissociated spleen cell cultures from normal mice. *J. Exptl. Med.* **126**:423.
63. Šterzl, J., J. Vesely, M. Jilek, and L. Mandel. 1965. Inductive phase of antibody formation studied with isolated cells. In *Molecular and Cellular Basis of Antibody Production*. J. Šterzl *et al.*, editors. Academic Press, Inc., New York. 463.
64. Ingraham, J. S. 1964. Dynamic aspects of the formation of serum antibody in rabbits. Exponential and arithmetic phases in the rise of titer following a re-injection of sulfanilazo bovine γ -globulin. *J. Immunol.* **92**:208.
65. Baker, P. J., and M. Landy. 1967. Brevity of the inductive phase in the immune response of mice to capsular polysaccharide antigens. *J. Immunol.* **99**:687.
66. Eiding, D., and H. F. Pross. 1967. The immune response to sheep erythrocytes in the mouse. I. A study of the immunological events utilizing the plaque technique. *J. Exptl. Med.* **126**:15.
67. Kennedy, J. C., J. E. Till, L. Siminovitch, and E. A. McCulloch. 1966. The proliferative capacity of antigen sensitive precursors of hemolytic PFC. *J. Immunol.* **96**:973.
68. Makinodan, T., and J. Albright. 1962. Cellular variation during the immune

- response: One possible model of cellular differentiation. *J. Cell Comp. Physiol.* **60** (Suppl. 1): 129.
69. Cooper, E. H. 1961. Production of lymphocytes and plasma cells in the rat following immunization with HSA. *Immunology.* **4**:219.
70. Harris, T. N., K. Hummeler, and S. Harris. 1966. Electron microscopic observations on antibody-producing lymph node cells. *J. Exptl. Med.* **123**:161.
71. Sercarz, E. E., and V. S. Byers. 1967. The XYZ scheme of immunocyte maturation. III. Early IgM memory and the nature of the memory cell. *J. Immunol.* **98**:836.
72. Fishman, M., J. J. van Rood, and F. L. Adler. 1965. The initiation of antibody formation by ribonucleic acid from specifically stimulated macrophages. In *Molecular and Cellular Basis of Antibody Production*. J. Šterzl *et al.*, Editors. Academic Press Inc., New York. 491.
73. Quastler, H. 1963. The analysis of cell population kinetics. In *Cell Proliferation*. L. F. Lamerton and R. J. M. Fry, Editors. F. A. Davis Company. Philadelphia. 18.
74. Talmage, D. W., and H. N. Claman. 1964. Cell potential: Its mutation and selection. In *The Thymus in Immunobiology*. R. A. Good and A. E. Gabrielson, Editors. Hoeber-Harper, New York. 49.
75. Nossal, G. J. V., G. L. Ada, and C. M. Austin. 1965. The antibody content of single antibody-forming cells. *J. Exptl. Med.* **121**:945.
76. Uhr, J., and G. Möller. 1968. Regulatory effect of antibody on the immune response. *Advan. Immunol.* **8**:81.
77. Nossal, G. J. V., C. M. Austin, and G. L. Ada. 1965. Antigens in immunity. VII. Analysis of immunological memory. *Immunology.* **9**:333.
78. Miller, J. J. 1964. An autoradiographic study of plasma cell and lymphocyte survival in rat popliteal lymph nodes. *J. Immunol.* **92**:673.
79. Landy, M., R. P. Sanderson, and A. L. Jackson. 1965. Humoral and cellular aspects of the immune response to the somatic antigen of *Salmonella enteritides*. *J. Exptl. Med.* **122**:483.

APPENDIX

The experimental data consist of the numbers of PFC scored in each labeling category and the time interval between the isotope injections. Their treatment to yield the length of the generation cycle depends on the nature of the kinetics of growth of the cell population. We describe two different ideal models of growth, chosen as extreme limiting examples, and with the understanding that real cell populations are unlikely to conform to these models in all respects. The first is steady-state growth and the second is exponential growth; these differ in the properties of the two cells produced by mitosis. In steady-state growth the two cells have different properties, and only one of them may reenter the growth cycle. In exponential growth both cells are identical and both reenter the cycle.

Steady-State Growth (Fig. 5a).—Wimber and Quastler (6) have described the use of the double label method in steady-state growth. They require that the cell population conform to the following assumptions: (a) it is asynchronous; (b) it has a negligible variation in its generation time; (c) it is in the steady state, remaining constant in size; (d) it remains constant in size because one of the two cells produced by mitosis leaves the cycle during G-1.

If a double label experiment is done using a short isotope interval, so that the tritium-

labeled cells have not left the G-2 period, as in Fig. 5d, the duration of the S period is given by (6):

$$H/C = t/s \quad (1)$$

where H is the number of tritium-labeled cells, C is the number of carbon-labeled cells, t is the time interval between isotope injections, and s is the duration of the S period.

The carbon-labeled cells identify the proportion of all the cells in the population sample

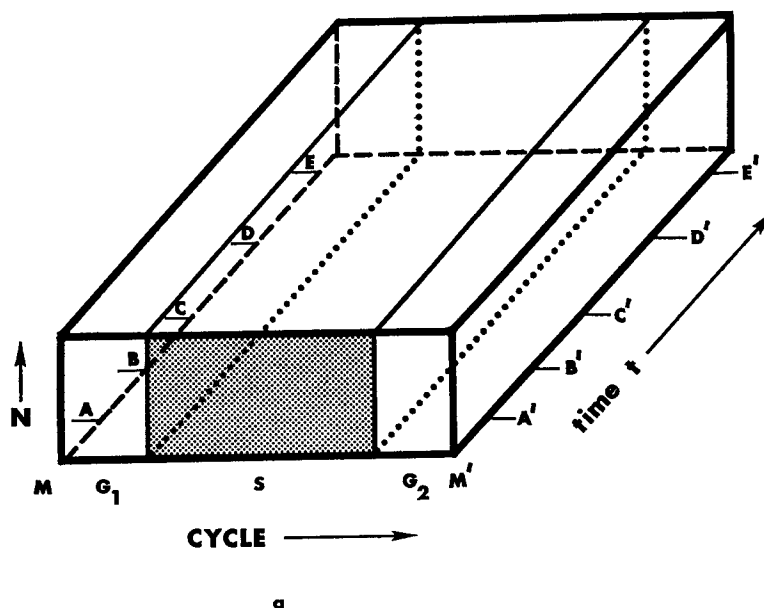


FIG. 5a. Steady-state generation cycle as a function of time. All axes are arithmetical. N is the number of cells present in the observed proliferating population; G-1, S, and G-2 are the phases of the generation cycle. Cells progress through the cycle from left to right until they reach mitosis, M' . In the steady state, only one of the two daughter cells reenters the cycle at M ; the other is lost from observation. Hence the total number of cells in the observed population remains constant with time. The shaded area indicates the tritium-labeled cells at the start of the double label experiment when time $t = 0$.

that are in the S period at the time of sacrifice (6, 7). Knowing the duration of the S period from Equation (1), the duration of the total generation cycle, T , is given by:

$$C/N = s/T \quad (2)$$

where N is the number of cells in the observed sample (the sum of H , C , and the unlabeled cells). For the results of Equation (2) to be valid, one must be certain that all the observed cells, N , are taking part in the growth cycle and that none are in a non-proliferative stage. This can be done by showing that no unlabeled cells are present when $t = g_1 + g_2$, where g_1 and g_2 are the duration of the G-1 and G-2 periods, respectively.

Graphical Estimate of the Generation Time.—An alternate method of estimating the genera-

tion time by graphic means is useful for several reasons. Because it treats only the proliferating cells, the generation time so measured will confirm the results of Equation (2) only if all cells in N are indeed proliferating. Of even greater interest, we will show that, unlike Equations (1) and (2), the graphic method is valid whether steady state or exponential kinetics occur.

The double label experiments are repeated, each with a progressively longer interval between isotope injections. At each step the tritium-labeled cells will have advanced farther through the cycle before the carbon label is applied (Fig. 5c-5h). The ratio of H/C is zero, when $t = 0$; it then rises and falls to zero again when $t = T$, since in the latter case the tritium cells have all returned to their initial position in the cycle. The duration of the generation cycle can be determined by noting the isotope interval required for H/C to rise, plateau, and then return to zero (Fig. 6). Equation (1) describes H/C when $0 \leq t \leq g_1 + g_2$. At the plateau, when $g_1 + g_2 \leq t \leq s$, the ratio is

$$H/C = \frac{g_1 + g_2}{s} \quad (3)$$

and when $s \leq t \leq T$, the ratio is

$$H/C = \frac{T - t}{s}. \quad (4)$$

These curves are shown in Fig. 6.

Exponential Growth.—It is clear that the assumptions of the steady state cannot be accepted *a priori* in the case of 19S antibody-forming cells. Therefore we derive additional equations describing the movement of the labeled cells in the event they grow with ideal exponential kinetics, the most extreme alternate model. These equations will show that the double-label data yield the duration of the generation cycle regardless of the model chosen.

We assume an ideal cell population in which: (a) there is asynchrony; (b) there is a negligible variation in the generation time; (c) there is exponential growth where both daughter cells of mitosis immediately reenter the generation cycle; (d) there is no inflow or outflow of cells by migration or death.

In such a population, Dawson and Field (8) have shown that the density function describing the distribution of cells at any point in the generation cycle is

$$f(N) = e^{-k\tau} \quad (0 \leq \tau \leq T) \quad (5)$$

where τ is the position in the cycle and $k = \ln 2/T$. This density function is shown by the closed curve LL'M'M in Fig. 5b. Since all cells arriving at mitosis (the line L'M') immediately reenter the cycle in doubled numbers at line LM, the total number of cells in the population, N , increases exponentially as a function of time and

$$N = N_0 e^{kt} \quad (6)$$

where N is the number of cells at time t and N_0 is the number of cells at $t = 0$. It is evident that Equation (6) may also be applied to subpopulations of N .

Since we must describe the labeled subpopulations of N both as a function of their position in the generation cycle and (as their size changes) as a function of time since the start of the experiment, these two functions are displayed in the three-dimensional diagram in Fig. 5b. For clarity, vertical sections parallel to the density function axes are made at various times (FF', GG', etc.) and are shown in Figs. 5i-5n.

A convenient experimental parameter is the observed ratio of tritium-labeled cells to carbon-labeled cells, H/C , and we formulate H/C as a function of the time interval t between isotope injections. These derivations depend to some extent on the relative duration of the

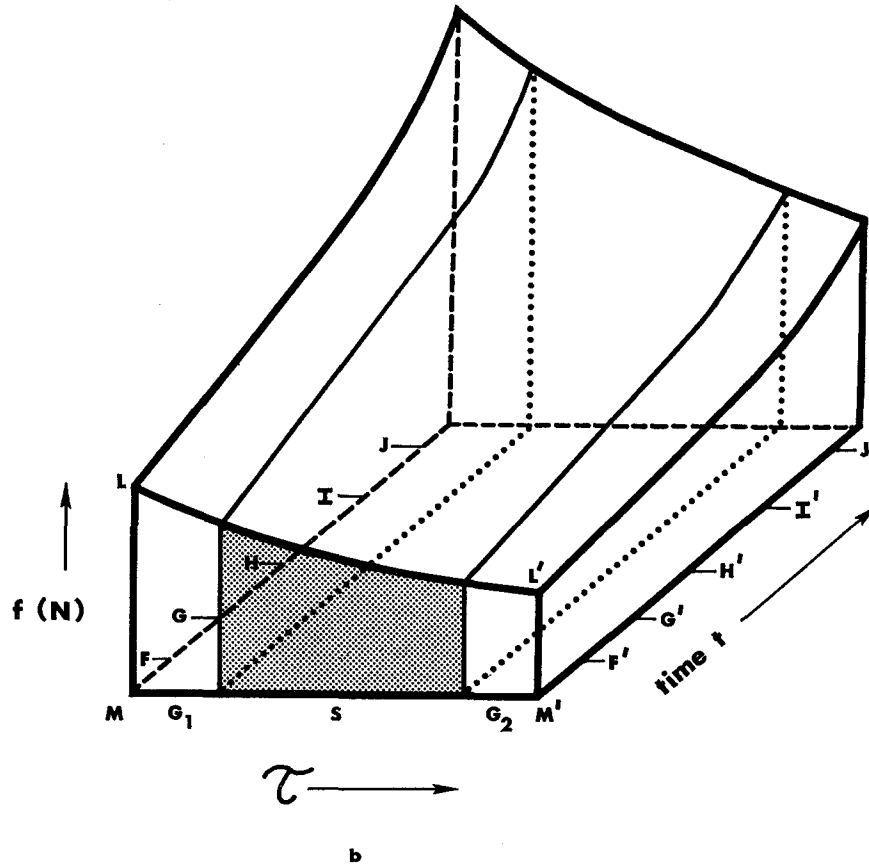


FIG. 5b. Exponential generation cycle as a function of time. All axes are arithmetical. G-1, S, and G-2 are the phases of the generation cycle; $f(N)$ and τ are defined in the Appendix. Cells progress through the cycle from left to right until they reach mitosis, the line $L'M'$. After division, the cycle begins again, both daughter cells reentering it at the line LM . Hence the total number of cells in the observed population increases exponentially with time. The shaded area indicates the tritium-labeled cells at the start of the double label experiment when time $t = 0$.

various phases of the generation cycle (6), and we first take the case in which $s > g_1 + g_2$ and $g_1 = g_2$. We neglect the duration of mitosis.

When $0 \leq t \leq g_2$: At $t = 0$, all the cells in the S period are labeled with tritiated thymidine, as shown by the shaded area in Figs. 5b and 5i, and they begin to move through the generation cycle. When carbon-labeled thymidine is given later at t , the number of tritium-labeled cells that can be observed in the G-2 period is represented by the shaded area in Fig. 5j. This area is

$$H = \int_{s+g_1-t}^{s+g_1} f(N) d\tau \tag{7}$$

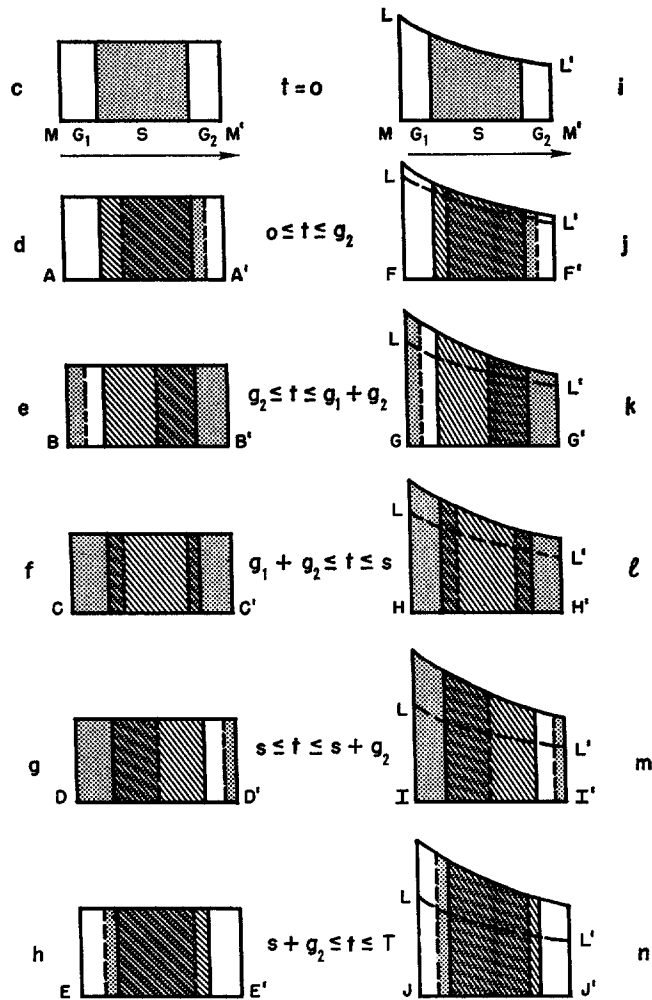


FIG. 5c-5h. Labeled subpopulations of the steady-state generation cycle as the isotope intervals are increased. The solid vertical lines are boundaries of the phases of the generation cycle. The dashed vertical bars are the boundaries of the tritium-labeled population as it passes through the cycle in time t . The carbon-14 label, indicated by the cross-hatching, always fills the S period and is given just before sacrifice at the times indicated at sections AA' , BB' , etc. in Fig. 5a. Tritium-labeled cells, shown as shaded areas, are scored as such only when they are in the G-1 or G-2 phases. Tritium-labeled cells in the S period are scored as carbon-labeled cells because the tritium label is obscured by the carbon label.

FIG. 5i-5n. Labeled subpopulations of the exponential generation cycle as the isotope intervals are increased. The carbon-14 label is given just before sacrifice at the times indicated at sections FF' , GG' , etc. in Fig. 5b, and is shown by cross-hatching. In contrast to the corresponding sections of the steady state, note that the number of cells in the population increases with time. This is shown by the dashed line LL' which indicates the size of the total population when time $t = 0$. Equations describing the changes in the sizes of the labeled populations are given in the Appendix.

and substituting from Equation (5)

$$H = \int_{s+g_1-t}^{s+g_1} e^{-k\tau} d\tau. \tag{8}$$

The number of carbon-labeled cells is always equal to the number of cells in the S period at time t , since the animal is killed shortly after the carbon label is injected. When $t = 0$, the

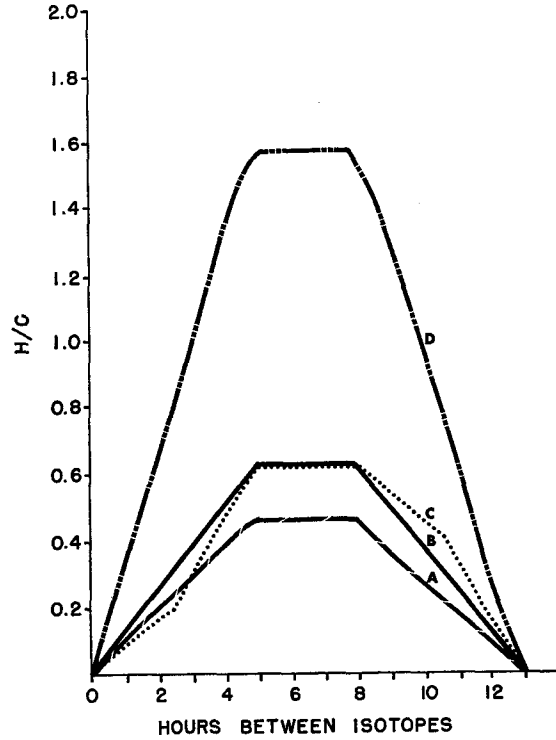


FIG. 6. Theoretical curves of the ratio of tritium cells to carbon-labeled cells as a function of the isotope interval. The curves are generated by equations given in the Appendix. *A* indicates exponential growth where $G-1 = 0$; *B* indicates the steady state; *C* indicates exponential growth where $G-1 = G-2$; *D* indicates exponential growth where $G-2 = 0$. In all cases the duration of the total generation cycle was taken to be 13 hr and that of the S period is assumed to be 8 hr. These values were inserted into the appropriate equations. Note that regardless of the type of growth assumed, all the curves have a common intercept on the time axis which is equal to the common generation time.

number of cells in the S period, N_{s_0} , is

$$N_{s_0} = \int_{g_1}^{s+g_1} f(N) d\tau \tag{9}$$

and substituting from Equation (5)

$$N_{s_0} = \int_{g_1}^{s+g_1} e^{-k\tau} d\tau. \tag{10}$$

At time t , however, the number of cells in the S period has increased, as shown by Equation (6). Substituting Equation (10) in Equation (6), the number of carbon-labeled cells, C , at time t is

$$C = e^{kt} \int_{g_1}^{s+g_1} e^{-k\tau} d\tau. \quad (11)$$

Dividing Equation (8) by Equation (11) and integrating, the required ratio is

$$H/C = \frac{e^{kt} - 1}{e^{kt}(e^{ks} - 1)}. \quad (12)$$

Integral equations giving the number of tritium-labeled cells at successive isotope intervals are derived by similar reasoning, but are omitted because of space limitations. The number of carbon-labeled cells is always given by Equation (11). The required integrated quotients of H/C are:

When $g_2 \leq t \leq g_1 + g_2$:

$$H/C = \frac{e^{kt} + e^{k(t-g_2)} - 2}{e^{kt}(e^{ks} - 1)}. \quad (13)$$

When $g_1 + g_2 \leq t \leq s$:

$$H/C = \frac{1 + e^{-kg_2} - 2e^{-k(g_1+g_2)}}{e^{ks} - 1} \quad (14)$$

Equation (14) indicates that the ratio remains constant during this interval.

When $s \leq t \leq s + g_2$:

$$H/C = \frac{1 + e^{-k(g_2+s-t)} - 2e^{-k(g_1+g_2+s-t)}}{e^{kt}(1 - e^{-ks})} \quad (15)$$

When $s + g_2 \leq t \leq T$:

$$H/C = \frac{2 - 2e^{-k(s+g_1+g_2-t)}}{e^{kt}(1 - e^{-ks})} \quad (16)$$

Equations (12-16) fully describe H/C as a function of all isotope intervals between $t = 0$ and $t = T$, when g_1 equals g_2 . Similar equations have been derived giving H/C as a function of the isotope interval in two extreme cases: when $g_1 = 0$, and when $g_2 = 0$. These equations will not be given, but the curves generated by them are shown in Fig. 6 together with the curves obtained from the steady-state equations and the five exponential equations shown above.

Generality of the Double Label Method.—These curves illustrate three practical points about the general utility of the double label method. First, there is little difference between the double label data obtained in steady-state growth and exponential growth (if in the latter case $g_1 = g_2$), but both these models can be readily differentiated from exponential growth in which either G-1 or G-2 are zero. Second, during the early isotope intervals there is a negligible difference between the curves of the steady state and exponential growth where $g_1 = g_2$. This

allows the use of Equations (1) and (2) to calculate the length of S and of T in either case, with only a small error if the isotope intervals are relatively short. Third, and most importantly, in all cases, (regardless of the model chosen) the length of the generation cycle can be estimated by measuring H/C in several experiments, each with a longer isotope interval, and by observing the isotope interval required for this ratio to return to zero. This time gives the duration of the generation cycle without further calculation.

We owe a great measure of gratitude to Dr. Alvin Essig for his review of the mathematical formulations and to Dr. Robert S. Schwartz for his generous counsel during this work.

FIG. 7a. Radioautograph of a hemolytic plaque with a tritium-labeled PFC in mitosis. Giemsa's stain. $\times 360$.

FIG. 7b. The same PFC as in Fig. 7a. The cell is in telophase with a prominent cleavage furrow. The plaque was prepared from the spleen of a mouse killed 2 hr after the *in vivo* injection of tritiated thymidine. Comparison of the sharply localized pattern of silver grains with that of Fig. 8b illustrates the ease with which tritium-labeled cells can be distinguished from carbon-labeled cells. Radioautographic exposure was 120 days. $\times 1300$.

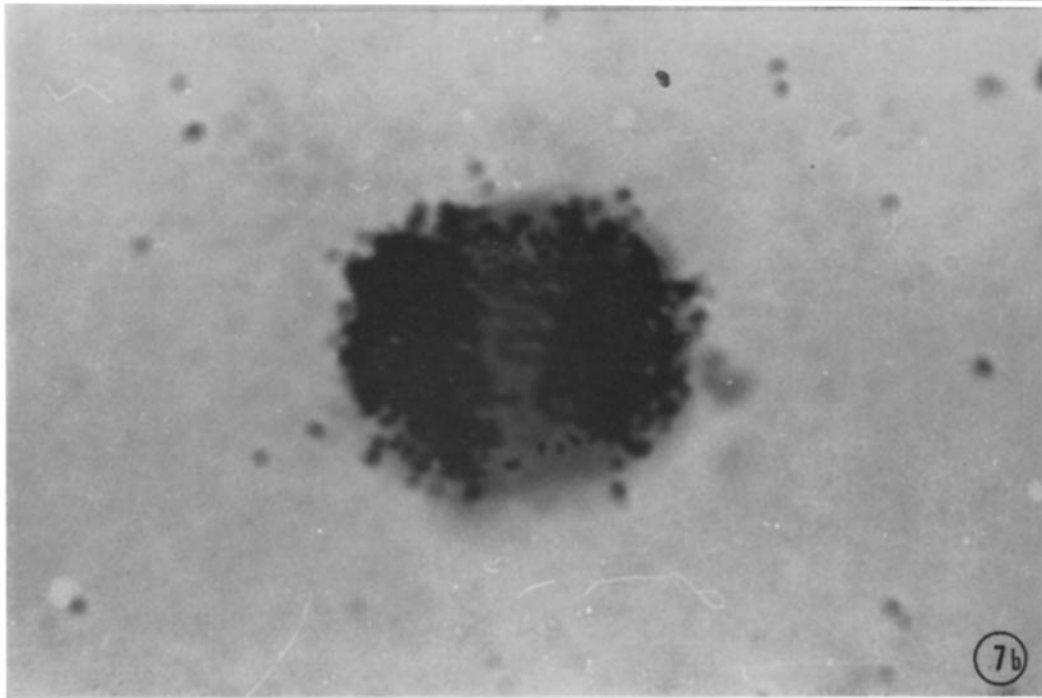
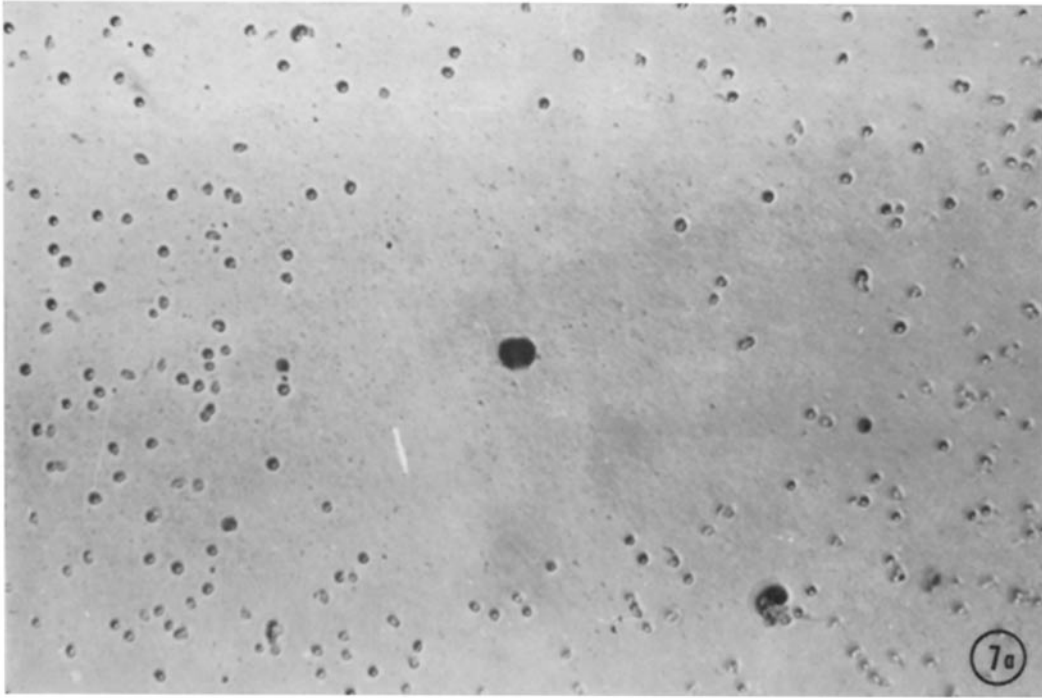


FIG. 8a. Radioautograph of a hemolytic plaque with a carbon-labeled PFC. Giemsa's stain. $\times 360$.

FIG. 8b. The same PFC as in Fig. 8a. By comparing the widespread pattern of silver grains with that of Fig. 7b, this cell is readily identified as being labeled with carbon-14. Note that if this cell had been labeled with tritium before the injection of carbon-14, as in Fig. 5d, the tritium label would be totally obscured; such doubly labeled cells are always scored as if they were labeled with carbon-14 alone. Radioautographic exposure was 150 days. $\times 1300$.

